

DANIELA FILIP<sup>\*)</sup>, DOINA MACOCINSCHI, GHIOCEL EMIL IOANID, STELIAN VLAD

“Petru Poni” Institute of Macromolecular Chemistry  
Aleea Gr. Ghica Voda 41 A, 700487, Iasi, Romania

## Multiblock segmented polyurethanes and polyurethane-ureas based on poly(ethylene oxide)/poly(propylene oxide)/poly(ethylene oxide) macrodiols. Synthesis and characterization

**Summary** — The amphiphilic behavior of poly(ethylene oxide)/poly(propylene oxide)/poly(ethylene oxide) block copolymers has been broadened by introducing new urethane-urea as well as poly(ethylene glycol) *co*-segments in polyurethane (PUR) and polyurethane-ureas (PURU) materials. Supermolecular organization and self-assembly was confirmed by electron microscopy transmission observations. The driving force for self-assembling is represented by the amphiphilic nature of these materials, the interactional segment length and stabilization through hydrogen bonding. FT-IR spectroscopy was used to investigate the hydrogen bonding related to phase segregation. Phase transitions and phase segregation was evidenced by DSC analyses. The relationship between structure and thermal stability was investigated by thermogravimetric analysis.

**Key words:** polyurethane, polyurethane-urea, multi-block structure, amphiphility, self assembly.

MULTIBLOKOWE POLIURETANY I POLIURETANO-MOCZNIKI O BUDOWIE SEGMENTOWEJ NA PODSTAWIE MAKRODIOLI POLI(TLENEK ETYLENU)/POLI(TLENEK PROPYLENU)/POLI(TLENEK ETYLENU). OTRZYMYWANIE I CHARAKTERYSTYKA

**Streszczenie** — Opisano sposób syntezy amfifilowych multiblokowych poliuretanów (PUR) i poliuretano-moczników (PURU) w wyniku wprowadzenia odpowiednich segmentów do łańcucha wymienionych w tytule makrodioli. Scharakteryzowano skład, strukturę oraz wartości  $M_w$  i  $M_w/M_n$  (tabela 1) uzyskanych PUR (2 typy) oraz PURU (również 2 typy). Przedyskutowano i porównano wyniki ich badania metodami FT-IR (rys. 5), derywatograficzną (rys. 1 i 2), różnicowej analizy termicznej (DSC, rys. 3, tabela 1), rentgenograficzną (rys. 4) i elektronowej mikroskopii transmisyjnej (rys. 6). Zinterpretowano zdolność do samorzutnego tworzenia agregatów przez opisywane produkty, wiążąc ją przede wszystkim z ich amfifilowym charakterem oraz stabilizacją poprzez wiązanie wodorowe. Wyniki uzyskane metodami DSC i FT-IR posłużyły do wyjaśnienia przebiegu zjawisk segregacji fazowej a także przemian fazowych.

**Słowa kluczowe:** poliuretany, poliuretano-moczniki, struktura multiblokowa, amfifilowość, zdolność do samorzutnej agregacji.

Progress in molecular engineering of polymeric and supramolecular entities with defined size, shape, architecture and chemical function indicate that self-assembly will play an important role in future technologies. Self-assembly plays essential role in biological matter and can be a source of inspiration for new artificial and simpler synthetic systems. New bioinspired materials and novel concepts in aiming at smart materials can therefore be created based on self-assembly and supramolecular interactions.

Multi-block copolymers such as segmented polyurethanes — provide a unique template for the design of synthetic materials with hierarchical microstructures [1, 2]. Amphiphiles (molecules consisting of parts having different chemical nature) find widespread applications

because of their unique ability to self-assemble and modify interfacial properties. Amphiphilic block copolymers consisting of water-soluble poly(ethylene oxide) (PEOX) and water-insoluble poly(propylene oxide) (PPOX) blocks are known under trade-name as Pluronics (or Poloxamers). These block copolymers have excellent biocompatibility being potential candidates in drug delivery systems and control release systems [3—7].

The introduction of urethane and urea structures and poly(ethylene glycol) fragments as *co*-segments might change the hydrophobic/hydrophilic balance of Pluronic copolymers thereby modifying the drug release properties. Modifications of PEOX-PPOX-PEOX copolymers are being explored for various applications [8—10]. The thermodynamic incompatibility of the polyurethane hard and soft segments drives microphase separation

<sup>\*)</sup> Corresponding author: dare67ro@yahoo.com

into hard domains stabilized by H-bonding between urethane and urea groups and soft segment domains.

The interplay between the microphase separation, the amphiphilic nature of the molecule and crystallization results in morphological richness of the self-assembly behavior. The main goal of the present work is to broaden the amphiphilic behavior of Pluronic-type copolymers by introducing new urethane/urea as well as poly(ethylene glycol) *co*-segments. Microphase segregation and self-assembly behavior of the resulted structures are investigated.

PUR-1:



PURU-2:



PUR-3:



PURU-4:



where:  $R_1$  and  $R_2 = -(CH_2)_6-$ ;  $R_3 = -(CH_2CH_2O)_n-[CH_2CH(CH_3)O]_m-(CH_2CH_2O)_n-$ ;  $R_4 = -(CH_2CH_2O)_s-$

## EXPERIMENTAL

### Materials

— Poly(ethylene glycol)-*block*-poly(propylene glycol)-*block*-poly(ethylene glycol) (macrodiol P<sub>123</sub>, PEOX<sub>20</sub>PPOX<sub>70</sub>PEOX<sub>20</sub>,  $M_n = 5800$  g/mol) was purchased from Sigma-Aldrich.

— 1,6-Hexamethylene diisocyanate (1,6-HDI, was purchased from Fluka and used as received).

— Polyethylene glycol (PEG600,  $M_n = 600$  g/mol) was purchased from Sigma-Aldrich.

— Chain extenders — 1,6-hexane diol (HD, 95 % purity) and 1,6-hexamethylene diamine (HDA, 99 % purity), both from Fluka — were used without further purification.

— *N,N*-Dimethylformamide (DMF, Fluka p.a.) served as solvent and dibutyl tin laurate (95 %, Aldrich) as catalyst.

### Synthesis

Four different polyurethanes (PUR) and polyurethane-ureas (PURU) were prepared by the typical two-step solution polyaddition in DMF. Firstly, the NCO-terminated prepolymer was prepared by dehydrating the macrodiol P<sub>123</sub>, and then the P<sub>123</sub>:PEG600 (1:1) mixture for 3 h at 90 °C under vacuum followed by the addition

of 1,6-HDI to the vigorously stirred dehydrated macrodiol. The diisocyanate/macrodiol molar ratio was maintained at 2:1. The reaction between diisocyanate and macrodiol was performed for 2.5 h under nitrogen at 90 °C in the presence of dibutyltin dilaurate. The temperature was lowered to 70 °C, the chain extender (HD, HDA) added and the reaction continued for a further 1.5 h. The resulting polymers were precipitated in water and dried under vacuum for several days. The general chemical structure of the synthesized amphiphilic multi-block PUR and PURU is presented below.

IR: 3300—3500 cm<sup>-1</sup> (>NH stretching), 2870—2970 cm<sup>-1</sup> (>CH<sub>2</sub>, -CH<sub>3</sub> stretching), 1718—1620 cm<sup>-1</sup> (>C=O stretching), 1100—1150 cm<sup>-1</sup> (C-O-C stretching).

<sup>1</sup>H NMR (DMSO-d<sub>6</sub>): 1.14 ppm -CH<sub>3</sub> (PPOX); 3—3.7 ppm -CH<sub>2</sub>-CH<sub>2</sub>-O- (PEOX), >CH-CH<sub>2</sub>-O- (PPOX); 2.5 ppm -CH<sub>2</sub>-CO-; 4.2 ppm -CH<sub>2</sub>-O-CO-; -NH-urethane groups 7.2 ppm, -NH- urea groups 5.7 ppm.

### Methods of testing

— The molecular weights were determined by using a GPC PL-EMD 950 evaporative mass detector instrument (solution in DMF, 1 %).

— Infrared Spectroscopy (FT-IR) was performed on a VERTEX 7 Instruments in the 600—4000 cm<sup>-1</sup> spectrum range with a resolution of 2 cm<sup>-1</sup> using thin films on KBr pellets.

— <sup>1</sup>H NMR spectra were registered using Bruker Avance DRX 400 Instrument (60 °C, DMSO-d<sub>6</sub> polymer solutions).

— The thermal stability was determined in air on a DERIVATOGRAF Q-1500 D apparatus (Hungary) under the following conditions: TGA scans were gathered at a ramping rate of 10 °C/min for samples with an initial weight of ca 50 mg in a 30—700 °C of temperature range.

— A Perkin-Elmer DSC-7 operated under nitrogen with a heating/cooling rate of 10 °C/min was used for thermal analysis for samples weighting 5—7 mg.

— The transmission electron microscopic (TEM) investigations were performed on a TESLA BS 513 A apparatus operating at a 80 kV voltage. Ultrathin films of polyurethane samples were prepared from 1 wt. % solution in *N,N*-dimethylformamide. Drops of the solutions were deposited on copper grids coated by a collodion thin film and then with carbon. Evaporation of the solvent was done at room temperature, under controlled conditions (supersaturated vapour atmosphere). Then, the grids were dried under high vacuum, for several days.

## RESULTS AND DISCUSSION

Compositional parameters, molecular weights ( $M_n$ : number-average molecular weights;  $M_w/M_n$ : polydispersity indices estimated from GPC) and glass transition

characteristics obtained from TG and DTG curves are presented in Table 2. It can be noticed that the introduction of urea groups promotes physical and chemical cross-linking therefore leading to increased thermal stability. The kinetics of the degradation process (degradation stage with a temperature value corresponding to the maximum rate of decomposition  $T_{max} \sim 400$  °C) was characterized by applying the calculation of the activation energy ( $E_{CR}$ ) and the order of decomposition reaction ( $n_{CR}$ ) by using Coats-Redfern method [15]. Higher values of  $E_{CR}$  and higher values of initial decomposition temperatures indicating higher thermal stability were found for urea based polymers. The curves for mass loss of the synthesized polyurethanes are presented in Fig. 1. The changes in activation energy as a function of conversion was followed by using the Levi-Reich kinetic analysis method [16]. The values of reaction order employed

**Table 1.** Compositional parameters, molecular weights ( $M_n$ ) and glass transition temperature ( $T_g$ ) values

Sample symbol	Soft segment (SSC)	Hard segment (HSC)	Composition <sup>a</sup> , % SSC	$M_n$ , g/mol	$M_w/M_n$	$T_g$ , °C <sup>b</sup>
PUR-1	P <sub>123</sub>	HDI HD	91	15 635	1.048	-68
PURU-2	P <sub>123</sub> /PEG600 (1:1)	HDI HD	87	41 905	1.419	-71
PUR-3	P <sub>123</sub>	HDI HDA	91	30 455	1.177	-69
PURU-4	P <sub>123</sub> /PEG600 (1:1)	HDI HDA	87	88 166	2.045	-66

<sup>a</sup>) Soft-segment concentration is defined as:  $SSC = (m_{pol} - m_{OH}) \cdot 100 / m_{total}$ , where  $m_{pol}$  is mass of polyol,  $m_{OH}$  is mass of hydroxyl groups and  $m_{total}$  is total mass of polymer; hard-segment concentration is  $HSC = 100 - SSC$ .

<sup>b</sup>)  $T_g$  — values were determined from the DSC second heating scan.

temperatures ( $T_g$  from DSC measurements) of the synthesized PUR and PURU are presented in Table 1.

**Table 2.** Thermal characteristics and kinetic parameters obtained from TGA data

Sample	Stages, °C	Mass loss, %	$T_{max}$ , °C	$E_{CR}$ <sup>*)</sup> , kJ/mol	$n_{CR}$ <sup>*)</sup>
PUR-1	I 165—240	15.3	400	19.5	0.2
	II 240—440	64			
PURU-2	I 160—220	5.3	400	28.7	0.0
	II 220—300	15.8			
	III 300—450	62.7			
PUR-3	I 185—440	86	410	58.4	0.6
PURU-4	I 240—440	80	405	76.8	0.9

<sup>\*)</sup> Symbols — see text.

Polyurethanes are known to be relatively thermally unstable materials — poly(ether-urethanes) being less thermally stable than polyester-based polyurethanes [11—14]. Their thermal stability depends on urethane/urea group ratio per unit volume, segment length and concentration. The thermal degradation of the synthesized multiblock polyurethanes is a complex process of at least two main degradation stages. The thermal

in the calculation were estimated by means of Coats-Redfern method. Variation of activation energy as a function of conversion ( $\alpha$ ) is presented in Fig. 2. The sharp drop of  $E_{CR}$  with  $\alpha$  suggests that urethane bonds per shorter PEG600 segments (PURU-2) promote the loss of the light degradation compounds [17] at lower conversions, whereas the close behavior shown by PUR-3 and PUR-4 indicates that physical and chemical cross-

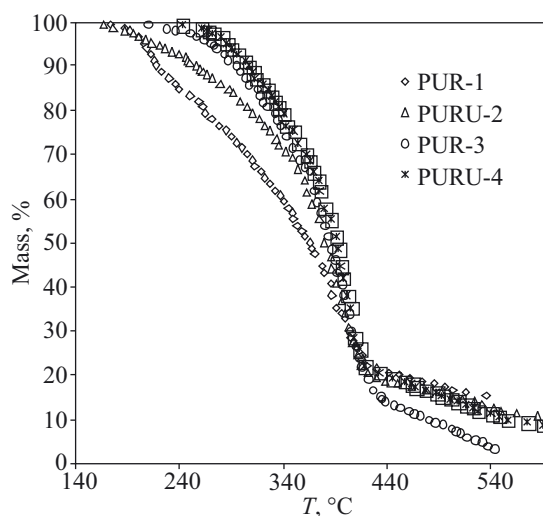


**Fig. 1.** Mass loss profiles of the polyurethane and polyurethane-urea samples

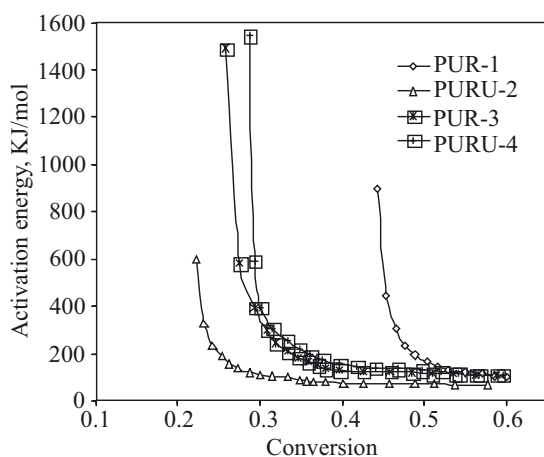


Fig. 2. Activation energy ( $E_{CR}$ ) vs. conversion curves of the polyurethane and polyurethane-urea samples

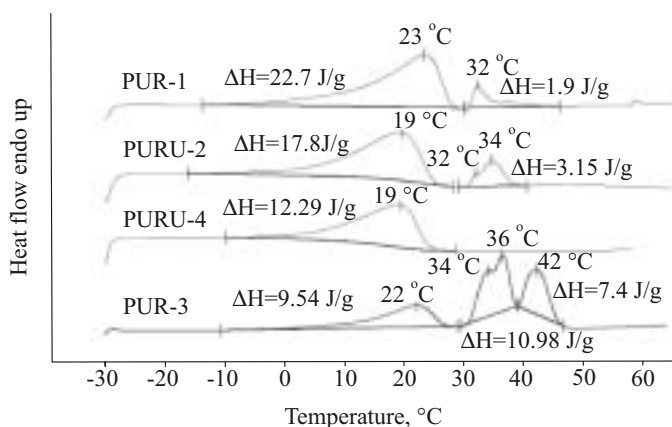


Fig. 3. DSC thermograms (first heating runs, 10 °C/min) of the polyurethane and polyurethane-urea samples

-linking determine the thermal behavior of urea-based polyether-urethanes.

The DSC thermograms of the polyurethanes and polyurethane-ureas are plotted in Fig. 3 (first heating scan, 10 °C/min). The values of the glass transition temperatures obtained from the second heating scans related to the soft segments are presented in Table 1. The values found for PUR-1 and PUR-3 are close to that found for the pure P<sub>123</sub> (-68 °C) suggesting phase separation between the soft and hard segments, whereas the  $T_g$  of PURU-2 is somewhat higher than the  $T_g$  found for pure PEG600 soft segments (-75 °C) and the  $T_g$  of PURU-4 is even higher due to urea and urethane physical and chemical network. The DSC scans shown in Fig. 3 in the first heating runs reveal multiple endotherms associated with multiblock structures and multiple levels of ordering. The melting peaks are well correlated with those found for the starting macrodiols, namely 22 °C for pure PEG600 and 23 °C, 38 °C for starting P<sub>123</sub>. The introduction of shorter PEG600 soft *co*-segments lowered the first endotherms, which corresponds to PEG crystalline phase of 19 °C (see PURU-2 and PURU-4).

The occurrence of a single peak (PURU-4) is attributed to urea and urethane hydrogen bonding generating physical and chemical cross-linking and in consequence preventing microphase segregation. At higher-melting temperatures endotherms associated with melting of the hard domains accompanied by thermal decomposition are observed in DSC scans which are not presented.

Wide angle X-ray diffraction patterns illustrating the semi-crystalline character of the obtained polyurethanes are presented in Fig. 4. In the case of PURU-2 the introduction of PEG600 *co*-segments enables the distinction of the crystalline peaks at  $2\theta$  — 19° and 23° — observed also for other Pluronics [8] and corresponding to PEG crystalline phase.

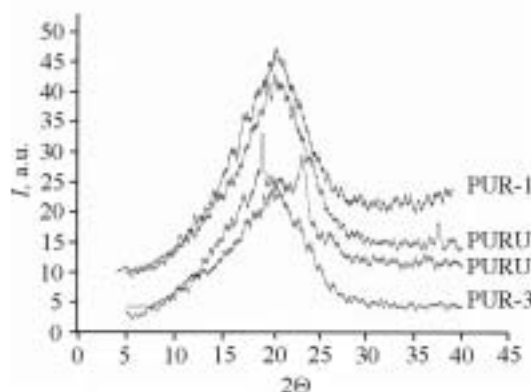


Fig. 4. X-Ray diffraction patterns of the polyurethane and polyurethane-urea samples

Hydrogen bondings, a complex phenomenon in polyurethanes, have been extensively studied using infrared spectroscopy [18–23]. Multiple hydrogen bonds are formed between the two kinds of proton donors (urethane and urea N-H groups) and three kinds of proton acceptors (urethane C=O, urea C=O, and ether C-O-C). The hydrogen bonding in urea polymers is stronger than in urethane polymers. Polyether-urethanes and polyether-urethane-ureas are characterized by hard-hard segment hydrogen bonding (NH---O=C) and hard-soft segment hydrogen bonding involving ether oxygen (NH---O) that represent the extent of mixing of the hard-soft phase. In general, the N-H groups free of hydrogen bonding have stretching vibrations located at higher frequencies (3400–3500 cm<sup>-1</sup>), whereas their counterparts involved in hydrogen bonding have stretching bands at lower frequencies (3100–3300 cm<sup>-1</sup>). The exact position depends on the strength of the hydrogen bonding formed and the local geometry. For amide I vibration, peaks assignable to free and hydrogen-bonded carbonyls located at lower wavenumbers are generally observed. The hydrogen-bonded carbonyls are formed by inter-urethane hydrogen bonding while most free carbonyls are formed when hard- and soft-segment mixing occurs, giving rise to hydrogen bonding between urethane and ether groups. The best fits performed for car-

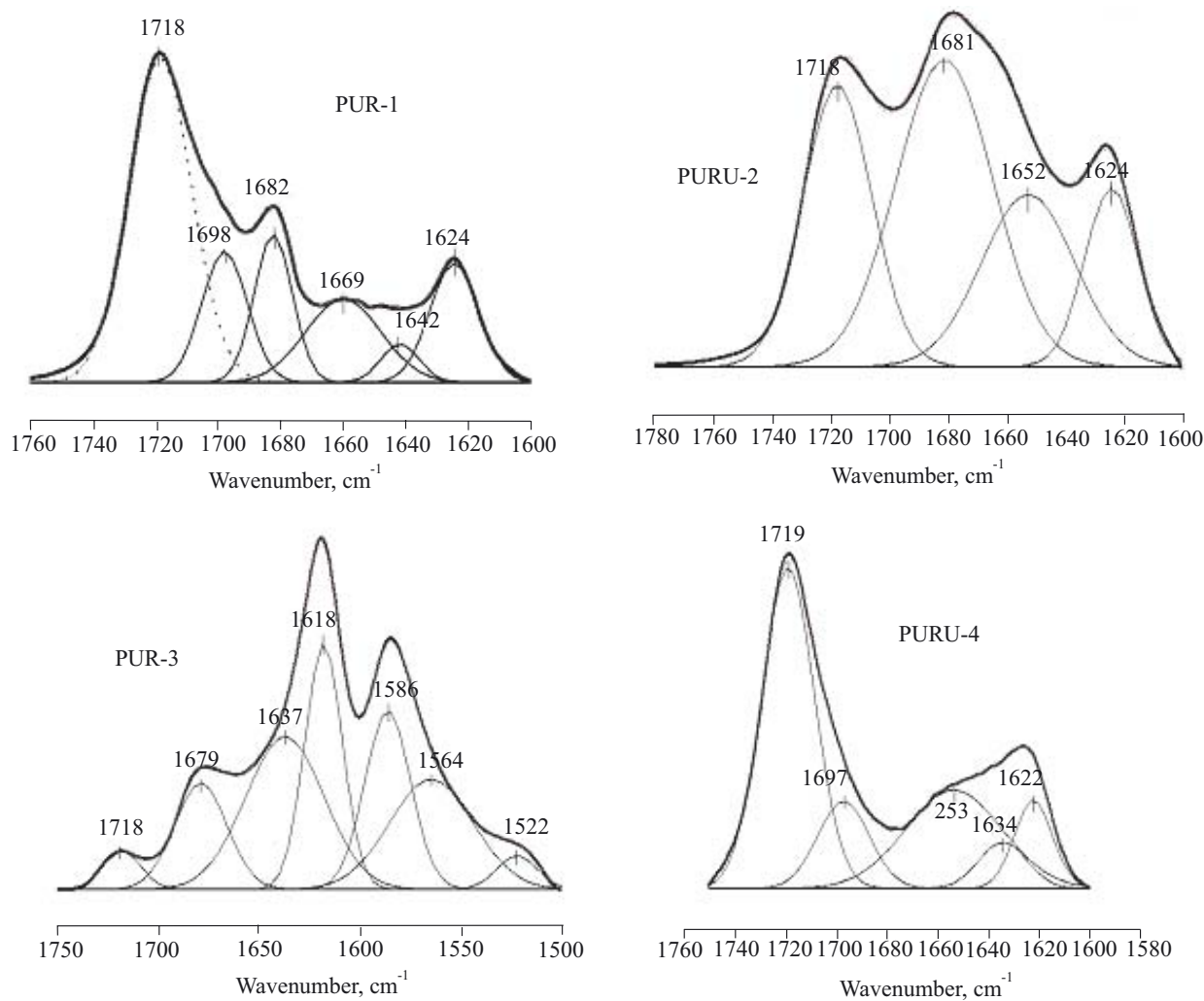


Fig. 5. FT-IR deconvolution peaks corresponding to C=O stretching region

bonyl stretching regions were obtained by using Gaussian function. Carbonyl stretching bands are resolved into multiple separate individual peaks. The deconvoluted peaks are presented in Fig. 5.

The peaks located at 1717, 1718 and 1719  $\text{cm}^{-1}$  are assigned to the free carbonyls as reported also in other papers [2], while the peaks located at lower wavenumbers are assigned to ordered and disordered forms of hydrogen bonding, corresponding to more or less ordered or disordered interfacial domains in the polyurethane and polyurethane-urea structure. The peaks located at 1618, 1622 and 1624  $\text{cm}^{-1}$  are assigned to strong inter-urethane or urea hydrogen bonding [23, 24]. In the case of PUR-3, the peaks located at 1522, 1564 and 1586  $\text{cm}^{-1}$  belong to amide II stretching region. There are remarked characteristic peaks such as free urea located around 1700  $\text{cm}^{-1}$ , 1697  $\text{cm}^{-1}$  for PURU-4 in our studies, and bidentate urea groups located around 1640  $\text{cm}^{-1}$  (1634 and 1637  $\text{cm}^{-1}$  for PURU-4 and PUR-3, respectively). A comparison of the spectra presented in the Fig. 5 shows that the polyether-urethanes are better correlated in the behavior of the carbonyl band relative to hydrogen bonding. In the case PURU-4 sample, the in-

tensity of the higher wavenumbers carbonyl band envelope is higher than that of the lower wavenumbers, while for the PUR-3 sample, the intensity of the higher wavenumbers band envelope is lower than the lower wavenumbers band envelope.

The fraction of hydrogen bonding  $[(X_b)_{CO}]$  in these polyurethanes and polyurethane-ureas could be obtained from the following equation [25]:

$$(X_b)_{CO} = [1 + 1.2(A_f)_{CO} / (A_b)_{CO}]^{-1} \quad (1)$$

where:  $(A_f)_{CO}$  and  $(A_b)_{CO}$  — the bond area of free carbonyl bonds and hydrogen-bonded carbonyl, respectively.

The results are presented in Table 3.

Table 3. Values of the fraction of hydrogen bonding  $[(X_b)_{CO}]$  and the ratio of peak intensity at 1624  $\text{cm}^{-1}$  to peak intensity at 842  $\text{cm}^{-1}$  for the studied polyurethane and polyurethane-urea samples

Sample	$(X_b)_{CO}$	Peak intensity at 1624 $\text{cm}^{-1}$ / peak intensity at 842 $\text{cm}^{-1}$
PUR-1	0.5	0.48
PURU-2	0.7	0.95
PUR-3	0.9	0.93
PURU-4	0.4	0.60

The multiple absorption bands reflect the complex properties of the hydrogen bonding in these poly(ether urethanes). Amide I stretch (carbonyl region) is most suited for studying hydrogen bond structures related to the degree of micro-phase separation and morphology. The micro-phase separation resulting in a hard-segment domain, soft-segment matrix and an interphase is a consequence of the immiscibility between the hard segment and the soft segment. The primary driving force for domain formation is a strong intermolecular interaction of hydrogen bonding between the hard-hard segments of urethane and/or urea linkages. Some hard segments are dissolved in the soft-segment matrix phase. An increase in this separation favours the inter-urethane, *i.e.* hard segment/hard segment hydrogen bonds.

The morphological feature of the segmented polyurethane is affected by many factors such as chemical composition, sequence length of the hard/soft segment and hydrogen bonding. For the PUR and PURU presented in these studies the small content of hard segment will result in their solubility and dispersion in the soft segment matrix, and hard segment (urethane/urea)/soft segment (ether) hydrogen bonding could become predominant. The chain length of the soft segment strongly influences phase separation, *i.e.* a long soft macromolecular chain will favour the micro-phase separation and crystallinity of the soft segment. On the other hand, urethane/urea groups per shorter soft segments, such as the introduction of PEG600 in the composition, will favour the hard domain ordering. Moreover, the introduction of the more polar urea groups will increase phase separation in hard domains and may induce a three-dimensional structure of the hydrogen bonding. Phase-separated hard domains in these polyurethanes are stabilized by hydrogen bonding of the hard segments.

The extent of hard segment separation was examined with FT-IR spectroscopy using the height ratio of a resolved peak attributed to inter-urethane hydrogen bonding, namely the peak around at  $1624\text{ cm}^{-1}$  found in all spectra, to a reference band located at around  $842\text{ cm}^{-1}$  (attributed to  $\nu_{\text{C-N}}$  stretching) [26]. The calculated ratios correlated with phase segregation in hard domains are also shown in Table 3. It is obvious that the high values of hydrogen bonding fractions correspond to high phase segregation in hard domains.

PEOX-PPOX block copolymers are remarkable for their ability to form a whole spectrum of self-assembled structures — from micellar solutions in water to lyotropic liquid crystals [27]. Their amphiphilic character arises from the difference in the hydrophobicities of PEOX and PPOX blocks in polar and nonpolar solvents. Their complex aggregation behavior involves unimers, oligomers, micelles and larger clusters, with a strong dependence on temperature and concentration [28, 29]. The formation of thermoreversible “gels” is a notable self-assembly feature of PEOX-PPOX block copolymers and is related to the close packing due to “hydrophobic” effect

of the micellar aggregates generating lyotropic liquid crystalline organization. H-bonding physical network or polymer entanglement might be also responsible for gel formation. The added salt exerts a strong influence on the behavior of the aqueous solution of the PEOX-PPOX polymers [28—32]. The solvent quality is a controlling factor of the block copolymer self-assembly. Non-aqueous solvents are also important in the elucidation of the self-assembly behavior of amphiphile molecules [33]. The immiscible segments of a block copolymer are known to facilitate phase separation in the solid state and micellar aggregates with the insoluble cores and soluble shells will form in a solvent which preferentially solvates one of the blocks. The resulting self-assembled materials can be ordered on the nanometer scale and is related to the length scale of associating polymer block segment. The microphase separation behavior in block copolymers becomes more complicated if one or more of the blocks are crystallizable. The process of crystallization of the respective blocks is expected to compete with microphase separation leading to the formation of confined as well as hierarchical structures [34, 35].

The size of the molecule (molar mass), composition, architecture, and concentration of the amphiphilic block-copolymers — all play a key role in aggregation behavior, size and shape of the microscopic self-assembled structures. There will therefore be an interplay between complex factors like crystallization, dissolution effect, amphiphilic segregation and interfacial association which will determine the self-assembled morphology. Self-assembled structures produced by amphiphilic molecules might possess various levels of organization that involves hierarchical steps, *i.e.* a complex large-scale supermolecular hierarchically organized structure being composed of smaller self-organized objects [36].

Electron microscopy is one of the best techniques for studying the morphology and determining mesomorphic structure and domain size. The morphology of block copolymer aggregates in non-aqueous solution has been investigated by TEM after transferring the non-aqueous solution to copper grids TEM images illustrating the self-assembly morphology of the polyurethane and polyurethane-ureas samples resulted after evaporation from 1 wt. % solutions in *N,N*-dimethylformamide are presented in Fig. 6. The formation of the amphiphile micelles or other aggregates depends on the interaction of the hydrophobic and hydrophilic segments as well as the interaction with the solvent. An additional strong effect can be expected from H-type interaction of urethane- and urea linkages which may influence the critical micelle concentration of the amphiphiles, the interaction with the solvent and the stabilization of the self-assembly.

Different nano-sized and submicrometer-sized geometric structures dependent on the synthesized material and different forms of coexistence (shape and size) of the aggregate micelles are obtained. The size of micelles is

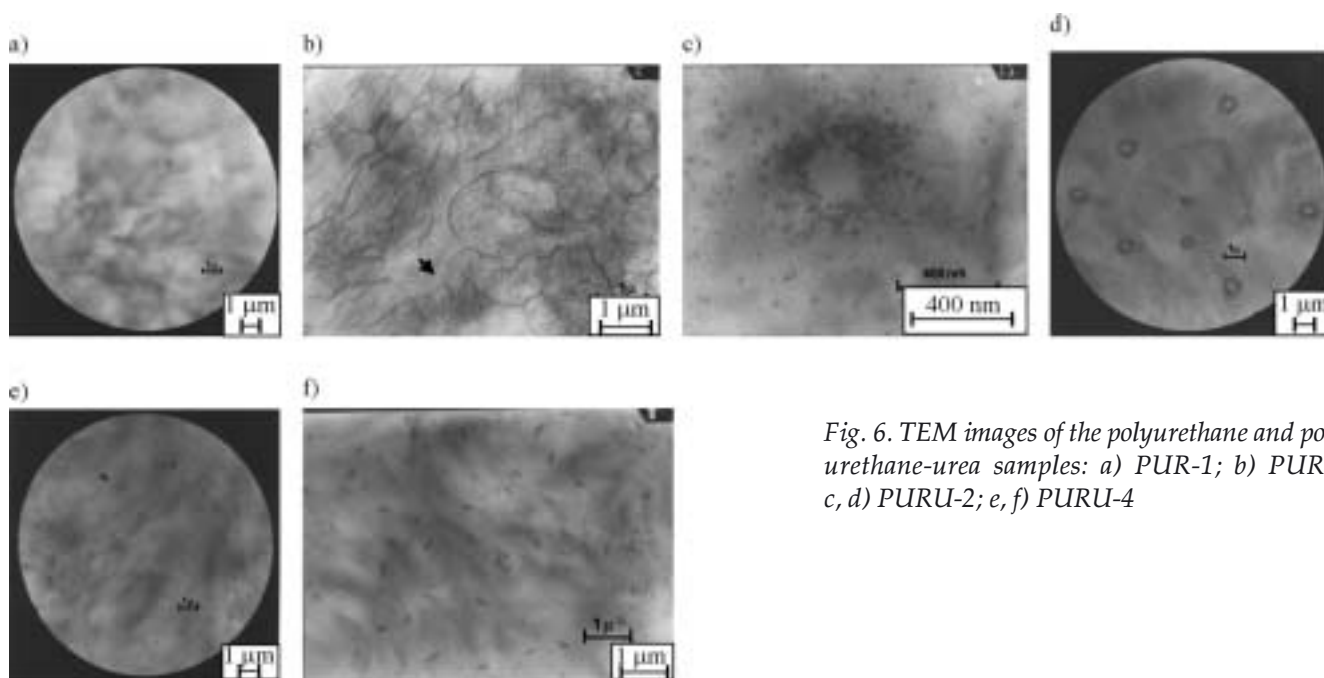


Fig. 6. TEM images of the polyurethane and polyurethane-urea samples: a) PUR-1; b) PUR-3; c, d) PURU-2; e, f) PURU-4

controlled by various factors, such as the length and nature of the core-forming segment and shell-forming chain. The determining role of polymer hydrophilic/hydrophobic balance on micelle morphology, the aggregation number and the solubilizing capacity of the system have been well-established [37, 38]. Cluster formation tendency is obvious for triblock copolymers self-assembly due to an enhanced interfacial chain packing as well as micellar close packing with the formation of an intermicellar network structure. In the case of PUR-1 (Fig. 6a), a nano-scale micellar organization can be observed. For PURU-2 (Fig. 6c, d), however, the self-assembly is more complex and hierarchical: the spherical micelles form micellar cluster aggregates which then pack closely in well-defined geometrically closed "ring" or "wheel-shaped" superassemblies. Larger micellar clusters are also observed. This cooperative interaction is specific to a gel state which is revealed in the background of the pictures. In the case of PUR-3 (Fig. 6b), a web of "worm-like" morphology is revealed and most probably also the additional coexistence of segregated mesomorphic domains marked with an arrow in the picture.

"Worm-like" morphology can be represented by a hierarchical form of associating "elongated" micelles with increasing concentration and micellar packing. In the case of PURU-4 (Fig. 6e, f) "rod-like" self-assembled micellar objects and larger micellar clusters are observed. Elongated micelles like rods may be associated with greater solubilizing capacity of the micellar system able to accommodate high values of aggregation number. Elongation of the hydrophobic chain leads to an increase of the hydrophobicity of the molecule and the equilibrium between dispersed amphiphiles is shifted towards aggregate superassemblies and gels. Linear H-bonding like urethane and urea may promote elon-

gated shapes of the amphiphile micelle, like rods or threads in a worm-like morphology. These images constitute a clear proof of manipulation of self-assembly. Such polymers could provide useful alternatives for solubilization of drug derivatives.

## CONCLUSIONS

The introduction of urethane and urea structures into an amphiphilic soft matrix has been performed, aimed at the manipulation of the supermolecular organization and self-assembly. The typical structural versatility of polyurethane/polyurethane-ureas materials resulted in different geometries and sizes (nano- and submicrometer scale) of the self-assembled structures as revealed by transmission electron microscopy observations. The driving force for self-assembling is represented by the amphiphilic character of the macromolecule, the interactional segment length and stabilization through hydrogen bonding.

## ACKNOWLEDGMENT

Authors gratefully thank the Ministry of Education and Research-Exploratory Research Projects, Code: PN-II-ID-PCE-988/2008 for financial support.

## REFERENCES

1. Koc Y., Hammond P. T., Lendl B., Gregoriou V. G.: *Macromol. Symp.* 2004, **205**, 191.
2. Korley L. T. J., Pate B. D., Thomas E. L., Hammond P. T.: *Polymer* 2006, **47**, 3073.
3. Barreiro-Iglesias R., Bromberg L., Temchenko M., Hatton T. A., Alvarez-Lorenzo C., Concheiro A.: *Europ. J. Pharm. Sci.* 2005, **26**, 374.

4. Chung H. J., Go D. H., Bae J. W., Jung I. K., Lee J. W., Park K. D.: *Curr. Appl. Phys.* 2005, **5**, 485.
5. Lin H.-R., Sung K. C., Vong W.-J.: *Biomacromolecules* 2004, **5**, 2358.
6. Park K. M., Bae J. W., Joung Y. K., Shin J. W., Park K. D.: *Colloid Surface B: Biointerfaces* 2008, **63**, 1.
7. Tian Y., Bromberg L., Lin S. N., Allan Hatton T., Tam K. C.: *J. Control. Release* 2007, **121**, 137.
8. Xiong X. Y., Tam K. C., Gan L. H.: *J. Appl. Polym. Sci.* 2006, **100**, 4163.
9. Ooya T., Ito A., Yui N.: *Macromol. Biosci.* 2005, **5**, 379.
10. Zhang Y., Lam Y. M., Tan W. S.: *J. Colloid Interf. Sci.* 2005, **285**, 74.
11. Petrovic Z. S., Zavargo Z., Flynn J. H., MacKnight W. J.: *J. Appl. Polym. Sci.* 1994, **51**, 1087.
12. Javni I., Petrovic Z. S., Guo A., Fuller R.: *J. Appl. Polym. Sci.* 2000, **77**, 1723.
13. Gopakumar S., Paul C. J., Gopinathan N. M. R.: *Mater. Sci.-Poland* 2005, **23**, 227.
14. Filip D., Macocinschi D.: *Polym. Int.* 2002, **51**, 699.
15. Coats A. W., Redfern J. P.: *Nature London* 1964, **201**, 68.
16. Reich L., Levi D. W.: *Makromol. Chem.* 1963, **66**, 102.
17. Cascaval C.: "Studiul polimerilor prin piroliza si cromatografie de gaze", Acad Romana, Bucuresti 1983.
18. Senich G. A., MacKnight W. J.: *Macromolecules* 1980, **13**, 106.
19. Lee H. S., Wang Y. K., Hsu S. L.: *Macromolecules* 1987, **20**, 2089.
20. Sun H.: *Macromolecules* 1993, **26**, 5924.
21. Ning L., De-Ning W., Sheng-Kang Y.: *Macromolecules* 1997, **30**, 4405.
22. Marcos-Fernandez A., Lozano A. E., Gonzales L., Rodriguez A.: *Macromolecules* 1997, **30**, 3584.
23. Garrett J. T., Xu R., Cho J., Runt J.: *Polymer* 2003, **44**, 2711.
24. Yilgor E., Yurtsever E., Yilgor I.: *Polymer* 2002, **43**, 6561.
25. Ge J., Wu R., Shi X., Yu H., Wang M., Li W.: *J. Appl. Polym. Sci.* 2002, **86**, 2948.
26. Balaban A. T., Banciu M., Pogany I.: "Aplicatii ale metodelor fizice in chimia organica" (Ed. Encicl St.), Bucuresti 1983.
27. Wanka G., Hoffmann H., Ulbricht W.: *Macromolecules* 1994, **27**, 4145.
28. Bahadur P., Li P., Almgren M., Brown W.: *Langmuir* 1992, **8**, 1903.
29. Mata J. P., Majhi P. R., Guo C., Liu H. Z., Bahadur P.: *J. Colloid Interf. Sci.* 2005, **292**, 548.
30. Wu Y. L., Sprik R., Poon W. C. K., Eiser E.: *J. Phys.: Condens. Matter* 2006, **18**, 4461.
31. Zheng L., Guo C., Wang J., Liang X., Bahadur P., Chen S., Ma J., Liu H.: *Vib. Spectrosc.* 2005, **39**, 157.
32. Demirors A. F., Eser B. E., Dag O.: *Langmuir* 2005, **21**, 4156.
33. Alexandridis P.: *Macromolecules* 1998, **31**, 6935.
34. Li C. Y., Tennesi K. K., Zhang D., Zhang H., Wan X., Chen E.-Q., Zhou Q.-F., Carlos A.-O., Igos S., Hsiao B.: *Macromolecules* 2004, **37**, 2854.
35. Maiti P., Nam P. H., Okamoto M.: *Macromolecules* 2002, **35**, 2042.
36. Sano M., Oishi K., Ishi-i T., Shinkai S.: *Langmuir* 2000, **16**, 3773.
37. Hurter P. N., Scheutjens J. M. H. M., Hatton T. A.: *Macromolecules* 1993, **26**, 5030.
38. Christov N. C., Denkov N. D., Kralchevsky P. A., Broze G., Mehreteab A.: *Langmuir* 2002, **18**, 7880.

Received 7 V 2009.